# ARTMAP NETWORK AND WAVELET ANALYSIS FOR FLAWS CHARACTERIZATION

M. C. Moisen[1, 2], H. Benítez[1], L. Medina*[1], E. Moreno[3], G. González[4], and L. Leija[4]
[1] DISCA-IIMAS-UNAM, México D. F.; México [2] UAG, Acapulco, México, [3] ICIMAF, La Habana, Cuba, [4] CINVESTAV, México D. F:, México

**Abstract:** Ultrasonic pulse-echo technique has been successfully used in a non-destructive testing of materials. This method aims to characterize the propagation path and/or to determine the physical properties of reflectors in terms of their location, size, orientation, and porosity. To perform ultrasonic non-destructive evaluation (NDE), an ultrasonic pulsed wave is transmitted into the materials using a transmitting/receiving transducer. The spectral analysis of the backscattered echoes has been widely used for flaws detection, frequency-shift estimation, and dispersive echoes characterisation. An innovative methodology is presented in this paper, in order to characterise flaws within the tested material

A pattern recognition technique based on ARTMAP network and wavelet transform is used as a digital processing tool that allows the geometry of flaws being determined. This technique consists of two non-supervised neural networks named ART2 (Adaptive Resonance Theory) and the Mexican hat wavelet transform.

An aluminium block with three man-made defects of circular geometries was scanned, by moving a single ultrasonic transducer along two perpendicular paths, producing two reflectivity maps containing the flaws information. The signal processing method proposed here used the received signals as follows: The total set of signals was split into two subsets, depending on the scanning path. The 10% of each subset was used to train an ART2 network, via the spectral information produced by the Mexican hat wavelet and the rest of them to validate the system. The ARTMAP network build a map field, since flaws are present in both axes, map field reproduced the flaws contour, based on the proper selection of vigilance and learning parameters.

**Introduction:** Ultrasonic flaw detection is an important technique to assure the quality of materials non-destructively. The goal for ultrasonic inspection is the detection, location and classification of internal flaws and defects. However, the detection capability is often limited by the interference noise produced by scatterers randomly distributed throughout the material. Spectral analysis is often adopted since the noise due to grain scattering exhibits variability in time domain.

Neural networks are well suited to signal classification in instrumentation. They have the ability to generalise and produce a result on the basis of incomplete data. For a neural network to reliably classify defects the training database must contain sufficient of each type of defect for the training operation to be effective. Where the type of defect is initially unknown it may also be possible to use automatic pattern classification and a self-organising network to generate the appropriate output states [1].

ARTMAP is a class of neural network architecture that perform incremental supervised learning of recognition categories and multidimensional maps in response to input vectors presented in arbitrary order [2].

ART stands for Adaptive Resonance Theory and was introduced by Grossberg in 1976. The main feature of all ART systems is a pattern matching process that compares the current input with selected learned category representation. ART is capable of developing stable clusters in response to arbitrary sequences of input patterns by self-organisation. ARTMAP extends the ART design to include both supervised and unsupervised learning. In ARTMAP, the chosen ART categories learn to make predictions in the form of mappings to output classes. Minimax learning rule enables the fuzzy ARTMAP system to conjointly minimise predictive error and maximise code compression or predictive generalisation.

ARTMAP [2] network has as main characteristic to perform incremental learning of recognition categories and multidimensional maps. This network is a supervised neural network associated to vector categories in order to construct a map. Two kinds of vectors are used, first vector is related to first ART network ($ART2_A$) and it is identified as unknown vector. Second vector is related to second ART network ($ART2_B$) and it is identified as predicted vector. Both ART2 networks perform a matching procedure in order to construct a map of those similarities between selected vectors.

The structure of this neural network consists of two ART2 networks [3]. Each ART2 network is independent in principle, although, first network modifies its vigilance parameter according to certain behaviour from MAP field.

Both ART2 networks follow the approach presented by Frank et al. (1998) [4]. This scheme is shown in Fig. 1.

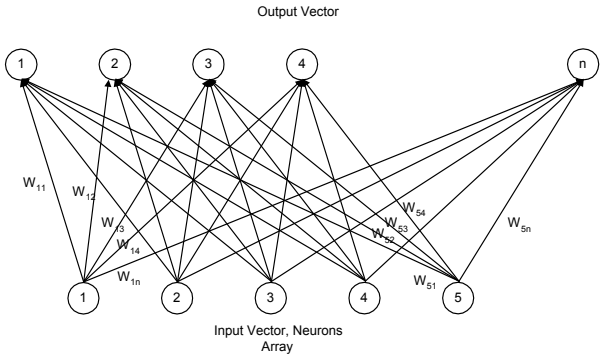


Figure 1. ART2 Network

The idea is to identify already classified patterns and categorize new patterns. This network is divided into two stages: a) bottom up (input-output) competitive learning and b) top-down (output-input) learning. The network stores patterns as sets of weights assigned to the paths connecting the input units to each of the output units. Presentation of an input vector causes the output units to be activated, the amount of activation depending on the similarity between the input vector and the stored pattern. Finding the nearest neighbour is simply a matter of deciding which output unit has been activated the most. The weights that connect each output unit to the input units represent the typical pattern of the class to which the output unit belongs. The weights that connect the input units to each output unit represent the same pattern, except that their values are normalised. The networks also have a mechanism for adding new category units to the output layer. This process is controlled by two parameters: the vigilance parameter and the learning parameter. The vigilance parameter, $\rho$, specifies how similar de input pattern is to be classified as belonging to the same category, and the learning parameter, $\eta$, controls the step size for weight adjustments.

The current input of the network is stated as **A**. This is normalized using the Euclidian media defined by

$$\mathbf{I} = \frac{\mathbf{A}}{|\mathbf{A}|} = \frac{\mathbf{A}}{\sqrt{\sum_{i=1}^{m} a_i^2}} \tag{1}$$

where $a_m$ is the *mth* element of A. The new generated vector I is used to perform another vector named as t based on

$$t_j = \sum_{i=1}^{m} w_{ij} i_i \tag{2}$$

where $w_{ij}$ is an element of weight matrix generated by previous pattern classification.

From $t_j$ element, a new vector is performed, stated as T. This vector represents the interaction between the already known weight matrix and the input vector. The maximum element from current *t* becomes the winner for this input vector then the stage bottom-up is completed. The maximum value of current *t* is compared against to vigilance parameter $\rho$ in order to determine if this current minimum value is closed to vigilance parameter. If this it so, the related winning vector $W_j$ is declared as representative pattern of the input A. Afterwards, $W_j$ is modified by

$$\mathbf{W}_J^{(new)} = \eta\mathbf{I} + (1-\eta)\mathbf{W}_J^{old} \tag{3}$$

where $\eta$ is defined as learning parameter.

Alternatively, if $\rho \leq t_J$ then a new pattern has been identified. Then a new vector $W_j$ is concatenated to weight matrix. This new vector is the current input vector I.

The selected network (ARTMAP Network) has the peculiarity of map field construction that represents the main characteristics of any pattern combination. This algorithm consists of two ART2A networks integrated to a map field as shown in Fig. 2.

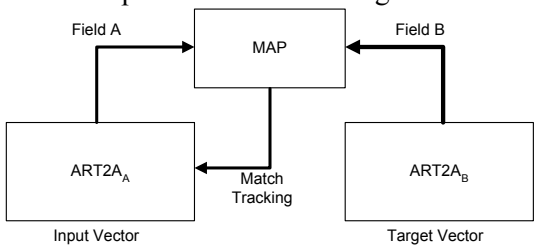


Figure 2. Structural construction of ARTMAP Network

Since the algorithm performed by each ART2 network has been defined, it is important to define how the map field is build. In this case both output vectors (from each ART2 network), named as $y_a$ and $y_b$ respectively, are send to map field. In there, the index of the winner neuron from first neural network is considered in order to select the respective vector from the related weight matrix from map field. Once the weight vector is selected, it is compared against output vector ($y_b$) from $ART2_B$ network. There are four possible cases with relation to map field selection.

$$x_{ab} = \begin{cases} y_b \wedge w_J^{ab} & \text{If } \textit{Jth} \text{ element from } y_a \text{ and } \textit{Jth} \text{ element from } y_b \text{ are active} \\ w_J^{ab} & \text{If } \textit{Jth} \text{ element from } y_a \text{ is active and } \textit{Jth} \text{ element from } y_b \text{ is not active} \\ y_b & \text{If } \textit{Jth} \text{ element from } y_a \text{ is not active and } \textit{Jth} \text{ element from } y_b \text{ is active} \\ \mathbf{0} & \text{If } \textit{Jth} \text{ element from } y_a \text{ and } \textit{Jth} \text{ element from } y_b \text{ are not active} \end{cases} \tag{4}$$

If

$$\left|x^{ab}\right| < \rho_{ab}\left|y^b\right| \tag{5}$$

then $\rho_a$ is increased until it is slightly larger than

$$\left|I \wedge w_J^a\right| I|^{-1} \tag{6}$$

where $W^{ab}$ is defined dimensional correct with respect to vectors $y_a$ and $y_b$. This matrix ($W^{ab}$) is initially declared by 1's and is modified according to $x_{ab}$ results.

The ART2A networks had been trained with time-scale information from the received signals. The time-scale process is based on wavelet analysis.

Wavelet analysis refers to a collection of methods that have found increasing use in signals processing, image analysis, and data compression.

The wavelet transformation of a time varying signal $x(t)$ consists of computing coefficients that are inner products of $x(t)$ against a family of "wavelets". These wavelets $\psi_{a,b}(t)$ are labelled by

scale and time location parameters $a$ and $b$. In continuous wavelet transform, the wavelet corresponding the scale $a$ and time location $b$ is

$$\psi_{a,b}(t) = \frac{1}{\sqrt{|a|}} \psi\left(\frac{t-b}{a}\right) \tag{7}$$

where $\psi_{a,b}(t)$ is the mother wavelet, which can be thought as a bandpass function. The continuous wavelet transform (*CWT*) is given by [5]

$$CWT_x(a,b) = \int x(t) \psi^*_{a,b}(t) dt \tag{8}$$

where * stands for complex conjugation.

Wavelet series (WS) coefficients are sampled CWT coefficients. Time remains continuous but time scale parameters are sampled on a "dyadic" grid in the time-scale plane ($b$,$a$). A usual definition is

$$C_{j,k} = CWT_x\big|_{a=2^j, b=k2^j} \quad \text{for } j,k \in Z \tag{9}$$

the wavelets are, in this case,

$$\psi_{j,k}(t) = 2^{-j/2} \psi\left(2^{-j} t - k\right) \tag{10}$$

and the original signal can be recovered though the following formula

$$x(t) = \sum_{j \in Z} \sum_{k \in Z} C_{j,k} \tilde{\psi}_{j,k}(t) \tag{11}$$

where $\tilde{\psi}_{j,k}(t)$ are also of the form of $\psi_{j,k}(t)$

A simple example of wavelet with infinite support is the so-called Mexican hat, defined by the second derivative of a Gaussian function as

$$\psi(t) = \left(1 - t^2\right) \exp\left(-t^2/2\right) = -\frac{d^2}{dt^2} \exp\left(-t^2/2\right) = \psi_{1,0}(t) \tag{12}$$

This wavelet has excellent localisation in time and frequency domains and clearly satisfies the admissibility condition. [6].

**Results**: All experiments were carried out with a Hydrophone scanning system (Specialty Engineering Associates SEA, CA, USA), two Personal computers (Pentium II, 128 RAM), and a digital oscilloscope (TDS-340 Tektronix, Oregon, USA). This system is able to control a motor to move the ultrasonic transducer along the x-axis, y-axis and z-axis with a 10$\mu$m step. The system can also store the waveforms, calculate the parameters and display a graphical representation of the experimental data.

In a typical experiment, the ultrasonic transducer and the phantom are immersed in a water tank (see Fig. 3), then the transducer is excited producing a pulse, the computer-controlled motor moves the transducer point by point, and an oscilloscope records the corresponding signal from each point and stores it. The transmission and triggering of the ultrasonic pulse of the transducer were controlled via a pulse-eco card MATEC SR9000 (Matec Instrument Companies, MA, USA).

The circular Krautkrammer (CR-RHP, GAMMA, 2.25X.50, BNC) ultrasonic transducer able to transmit a pulse at 2.25 MHz has been used. The phantom is an aluminium block of 70x70x40 $mm^3$, with three man-made circular flaws diagonally located.

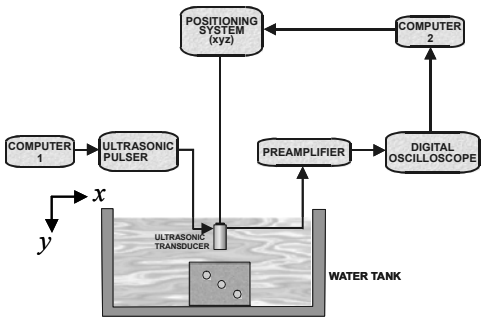


Figure 3. Experimental Setup

The proposed ARTMAP architecture was applied to simulated and real data. The simulation of received signals and the ARTMAP algorithm had been developed on MATLAB platform. The ARTMAP algorithm was tested when the ART2A$_A$ and ART2A$_B$ networks were trained with and without wavelet information.

In order to test the ARTMAP network algorithm, simulated signals were used. Those signals with additive white noise represent the scanned medium along *x* and *y*-axis, where three point-in-homogeneities are diagonally located. The received signals were split into two different sets: the first set is related to the *x*-axis scanning direction and the second to the *y*-direction, as shown in Figure 4.

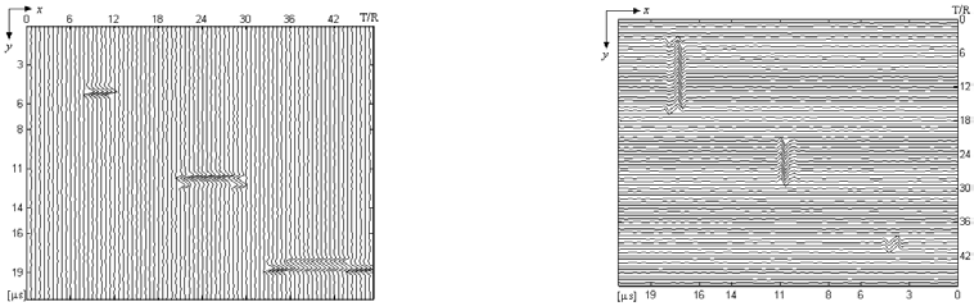


(a) (b)

Figure 4 Simulated received signals: a) along *x*-axis and b) along *y*-axis.

The ARTMAP algorithm was first applied to the normalised (see eq. 1) received signals in order that ART2A$_A$ and ART2A$_B$ patterns were computed and the map image produced as shown in Figure 5. The learning and vigilance parameters values are shown in Table 1

When the signals are wavelet transformed using the Mexican hat mother wavelet (eq. 12) and normalised, the output patterns of ART2A$_A$ and ART2A$_B$ and the autoregressive map are shown in Figure 6.

The main differences of ARTMAP outputs when the network is trained with and without wavelet analysis are: a) the noisy patterns in Figures 5a and 5b are cleared when Mexican hat wavelet transform is included in the digital process (see Figures 6a and 6b), and b) the vigilance parameter of ART2A$_B$ is slightly diminished, reducing the number of patterns in the wavelet-ARTMAP network (see Table 1).

The same digital process was applied to real data. Two perpendicular B-scans were made acquiring two sets of received signals as shown in Figure 7. Each signal was wavelet transformed and normalised to compute the input vector of each ART2A networks. Those vectors generate the patterns that produce the map of similarity among them as shown in Figure 8.

Since the real data is quite noisy, due to reflections coming from in-homogeneities, bottom of water tank, impurities, among others, the number of patterns in ART2A$_A$ and ART2A$_B$ is quite

large, compared to the patterns produced when simulated data is used in the digital process. Also the vigilance and learning parameters are varied as shown in Table 1.

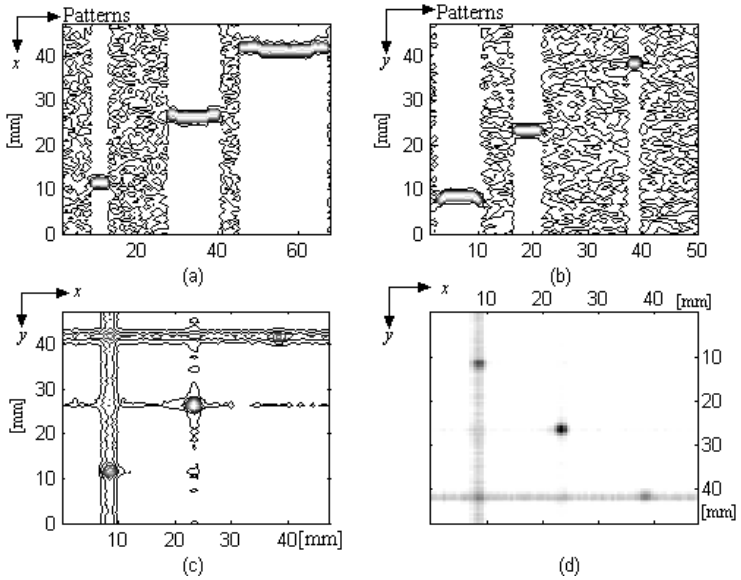


Figure 5. Patterns and images of ARTMAP process: a) ART2A$_A$, b) ART2A$_B$, c) contour, and d) image of $x_{ab}$.

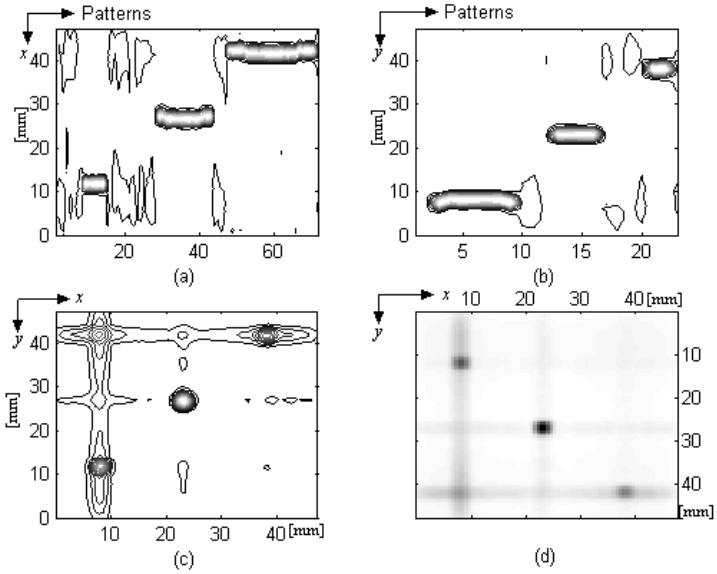


Figure 6. Patterns and images produced by ARTMAP-wavelet process: a) ART2A$_A$, b) ART2A$_B$, c) contour, and d) image of $x_{ab}$.

**Discussion:** Present results show how this composite algorithm can overcome noise presence inherent to those processed signals. In fact, there are several variables to be considered such as the selection of the mother wavelet, the vigilance and learning parameters and the structure of the network itself.

It has found, on simulation and experimental basis, that Mexican hat wavelet presents suitable results respective to the noise inherent in the studied signals. Figure 5c and Figure 6c depicted clearly the intersections of selected patterns from ART2A networks. It is important to highlight that this intersections are defined as part of the construction of the map within the ARTMAP

network. This map does not produce those intersections because the spatial relationship of the input signals, it is constructed based on similar locations of the patterns.

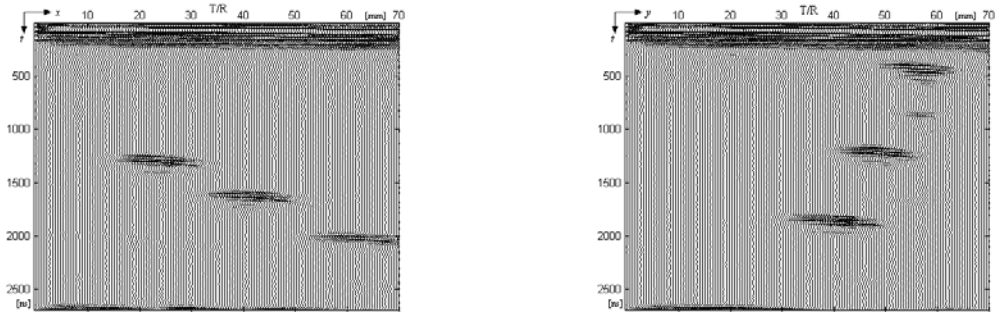

(a) (b)

Figure 7. B-scan experimental data: (a) along *x*-axis and b) along *y*-axis

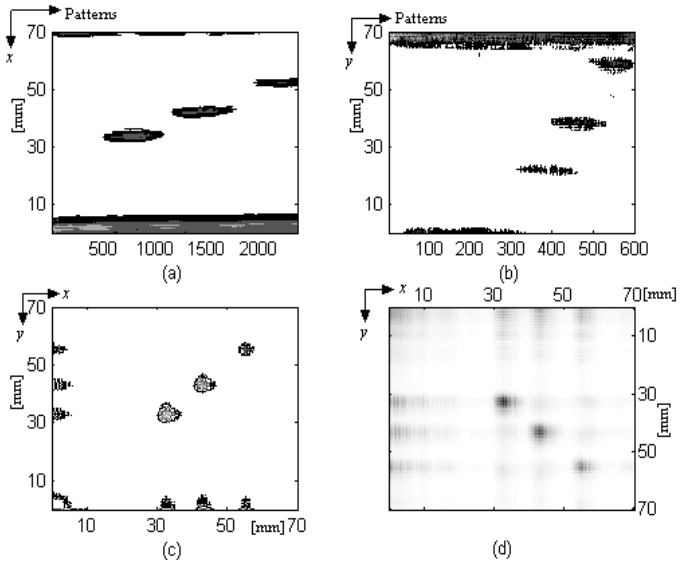


Figure 8. ARTMAP output for real data: a) $ART2A_A$ patterns, b) $ART2A_B$ patterns, c) contour and d) image of the digital process result.

| Parameter | (a) | (b) | (c) |
|---|---|---|---|
| $\rho_a$ | 0.800 | 0.800 | 0.650 |
| $\eta_a$ | 0.750 | 0.750 | 0.751 |
| $\rho_b$ | 0.800 | 0.770 | 0.872 |
| $\eta_b$ | 0.750 | 0.750 | 0.750 |
| $\rho_{ab}$ | 0.750 | 0.790 | 0.700 |

Table 1. ARTMAP parameters values when normalised input vectors are: a) raw signals and b) normalised wavelet transformed signals.

**Conclusions:** This paper has presented a novel approach for non-destructive testing based on a combined algorithm of wavelet transform and ARTMAP network. The autoregressive map is built considering the following: a) the orthogonal characteristic of the two B-scan, and b) the selected neural network that has the advantage of map construction by the intersection of common patterns.

When simulated signals with additive white noise are used as input vector of the ART2A networks the number of pattern due to noise is reduced when the signals are wavelet transformed, however the resulting map is not clearly affected. However if real data is the input vector the number of patterns produced by the ART2A networks is drastically diminished when Mexican hat is applied to the received echoes. Even though that this number is larger than 2000 for the $ART2A_A$ case. It can be reduced, therefore the time consuming process, if the echoes coming from the faces and bottom of the phantom are neglected.

This technique has presented not only flaw location it has produced flaw characterisation as a result of map construction. This may enhanced the idea of multidimensional pattern recognition.

Further studies are pursued in terms of a NDT autonomous procedure where the ARTMAP network can separate several types of flaws as well as determine certain geometric characteristics of them. Alternatively, further work is pursued in order to incorporate wavelet decomposition characteristics into ARTMAP learning procedure as well as map construction.

**References:**

[1] Margrave F. W., Rigas K., Bradley D. A., Barrowcliffe P., "The Use of Neural Network in Ultrasonic Flaw Detection", Measurement 25, pp. 143-154, 1999.

[2] Carpenter G. A., Grossberg S., Markuzon N., Reynolds J. H., Rosen D. B., "Fuzzy ARTMAP: A Neural Network Architecture for Incremental Supervised Learning of Analog Multidimensional Maps", IEEE Trans. Neural Network 3, pp. 698-713, 1992.

[3] Carpenter G. A., Grossberg S., "The ART of Adaptive Pattern Recognition by a Self-Orginizing Neural Network", IEEE Computer 21, pp. 77-88, 1988.

[4] Frank T., Kraiss K. F., Kuhlen T., "Comparative Analysis of Fuzzy ART and ART-2A Network Clustering Performance", IEEE Trans. Neural Network 9, pp. 544-559, 1998.

[5] Akay M., "Time Frequency and Wavelets in Biomedical Signal Processing", IEEE Inc., New York, 1998

[6] Debnath L., Wavelet transforms & their applications", Birkhauser, Boston 2002.